Analysis of Clothing Pressure on the Human Body

Takaya Kobayashi, Shuya Oi, Masami Sato

Mechanical Design & Analysis Corporation

Masato Tanaka

Keio University

Yumiko Isogai, Kenji Furuich, Sonoko Ishimaru, Chisato Nonomura

TOYOBO Co., Ltd.

Abstract: This paper describes the development of knitted fabric models for finite element analysis to simulate the large deformation behavior of garments and their clothing pressure distribution on the human body. In this study, for the modeling of cloth materials, two analytical approaches are investigated: a rebar layer model combined with isotropic hyperelastic shell elements and an anisotropic hyperelastic material model with a polyconvex strain energy function defined by the UMAT user-subroutine. These material models are implemented in the four-node shell element S4R of Abaqus/Standard and achieved adequate performance in predicting the deformation behavior of fabric test specimens and the computation of the contact pressure distribution on the human body caused by clothing. This study presents a fully automatic and seamless simulation of the clothing process for pantyhose and T-shirts, and the results show a good agreement with the experimental results.

Key words: Knitted Fabric, Shell, Buckling, Rebar, UMAT, Artificial damping

1. Introduction

The comfort provided by clothes is a key element that directly affects the human psychology as well as physiology in all environmental conditions. The primary elements that compose comfort include the temperature and humidity conditions inside the clothes, which are referred as the "clothing enclosure climate;" clothing pressure generated when the human body is pressed under clothes; and the feeling of clothing largely influenced by the materials. Among these elements, the benefits of clothing's pressure are comfort, as well as an improvement in motor skills, a reshaping of the body, and the medical changes in the nervous and circulatory systems. Still, there are cases in which the clothing pressure should be lowered as much as possible.

In order to realize moderate clothing pressure, the most common approach in the sewing process is to repeat modified sewing repeatedly based on the examinees' sensory impression. Through this sewing process, the fittings by examinees are an indispensable step. However, if subtle designs are required, this process may not be a highly efficient way to improve clothing. Also, the sensory impression tests cannot provide strict quantitative data, so now more accurate evaluation measures are needed.

For measuring the clothing pressure, sensing elements are commonly inserted between the human body and the clothes. However, practical measurements are often restricted by available sizes of the pressure sensors and the available measuring points on a human body. Furthermore, clothing conditions deviate widely from tight to loose. Under these circumstances, mapping the clothing pressure distribution all over a human body's surface remains a hard task. Even if the pressure data is obtained, it may not good enough to cover the design of the clothes. Since the interaction effects between the human body and clothes, e.g., wrinkles, slackness, and tightness, cannot be evaluated only from the clothing pressure data, further information about the deformation of the clothes is necessary.

Recent innovations in the workability of clothing materials enable us to utilize the interaction between the human body and clothes to determine any assistance for physical performance. Especially in high-value-added application fields, such as sports and medical services, the demand for better clothing is increasing greatly. For consumer products, such as underwear, the cascading effect from this high technology has broad applications and uses for direct benefits that improve daily life. In response to the recent trends, the authors sought an efficient technique for predicting the clothing process using finite element analysis.

In order to simulate the clothing process, it is necessary to represent the deformation behavior of the fabric in terms of available material models. The cloth materials are complicated products made from a spinning, weaving, or knitting process. Instead of modeling the yarns, the macroscopic deformation of the yarns, after they are knitted into clothing, can be determined. Either way, they present their complex behavior due to the combined effects of the highly nonlinearity and anisotropic properties. In this study, two analytical approaches are investigated: a rebar layer model combined with isotropic hyperelastic shell elements (Ishimaru et al. 2010) and an anisotropic hyperelastic material model with a polyconvex strain energy function defined by the UMAT user-subroutine (Tanaka et al. 2010).

For the simulation of the clothing pressure, a study using isotropic FEM and FDM was done by X. Zhang et al. (2004). In this study, Abaqus, the general purpose FEM, is used for its powerful nonlinear analysis capability to overcome the difficulties of the material modeling and the large deformation of the clothing. The study accomplishes a fully automatic seamless simulation of the clothing process for garments such as pantyhose and T-shirts. The results from this study show a good agreement with the experimental results.

2. Material model of knitted fabric

Cloth materials are generally classified into woven and knitted fabrics. In this study, the knitted fabric with a more complicated structure is the target (Figure 1). The knitted fabric has a fiber structure with yarns mutually twined into loops. The respective directions of the wale and course are determined according to the orientation of yarns. Figure 2 shows the deformed shapes of the actual knitted fabric stretched in the course direction. In the initial stage, the loops are deformed and, in the latter stage, the yarns are elongated. Consequently, it can be assumed that the measured load increment will increase gradually as the yarn is stretched. Therefore, the respective stiffness along each orientation is governed by the knitting pattern. It is a common that the relationship between the measured load and the displacement shows anisotropic behavior. In this study, the nonlinearity and anisotropic characteristics exhibited by knitted fabrics are modeled with two approaches: a rebar layer model and an anisotropic hyperelastic material model. The following sections discuss these approaches.

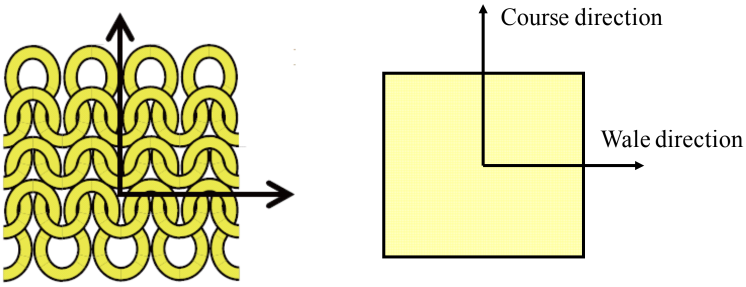

Figure 1. Schematic model of knitted fabric.

Figure 2. Elongation of knitted fabric.

2.1 Formulation of rebar layer model

The rebar layer model was built using an isotropic hyperelastic shell element for the matrix of the cloth material, combined with a rebar layer defined on the matrix along the wale and course (Figure 3), (Ishimaru et al. 2010). The isotropic matrix follows the neo-Hookean hyperelastic material model. The potential energy of the neo-Hookean hyperelastic model W_{neo} is expressed as

$$W_{neo} = C_{10}(\lambda_1^2 + \lambda_2^2 + \lambda_3^2) \tag{1}$$

where C_{10} is the material parameter and λ_i $(i = 1, 2, 3)$ are principal stretch ratios. $\lambda_1^2 + \lambda_2^2 + \lambda_3^2$ is equivalent to the first strain invariant I_1. An element-based rebar layer is defined as the reinforcing member arranged in the specified in-plane orientation of the shell element. The rebars represent the uniaxial reinforcement along the wale and course (Figure 3). The rebars' material properties are given by the hypoelastic model with a Young's moduli E_{wale} and E_{course}, which give the strain-dependent nonlinear axial stiffnesses. The elasticity tensor D_{ijkl} is obtained by the superposition of the isotropic matrix and rebars as follows;

$$D_{ijkl} = \frac{\partial^2 W_{\mathrm{neo}}}{\partial \varepsilon_{ij} \varepsilon_{kl}} + E_{\mathrm{wale}} \delta_{1i} \delta_{1j} \delta_{1k} \delta_{1l} + E_{\mathrm{course}} \delta_{2i} \delta_{2j} \delta_{2k} \delta_{2l}, \qquad \{i, j, k, l\} = \{1, 2, 3\} \tag{2}$$

where directions 1 and 2 denote the wale and course directions, respectively. Direction 3 is perpendicular to the wale and the course directions and δ_{ij} represents the Kronecker's delta. E_{wale} and E_{course} take the form of a series in terms of ε_{11} and ε_{22}, respectively.

$$E_{\mathrm{wale}} = \sum_{i=0}^{N} c_i \varepsilon_{11}^{i} \tag{3}$$

$$E_{\mathrm{course}} = \sum_{i=0}^{N} d_i \varepsilon_{22}^{i} \tag{4}$$

The material parameters C_{10}, c_{i}, N, and d_{i} (i=1,・・・, 6) are determined through uniaxial tensile tests in three directions: wale, course, and bias. This rebar layer model is implemented via Abaqus/Standard in which the isotropic matrix part is represented by the shell element S4R. Its reinforcement is modeled with the rebar layers' capability. Consequently, this provision allows the shell element to exhibit nonlinear and anisotropic elastic behavior. The shell element, as the matrix of the rebar layers, exhibits the Poisson's effect due to its isotropic hyperelasticity, but the respective axial property of the wale and the course defined as the reinforcing rebar do not relate to each other.

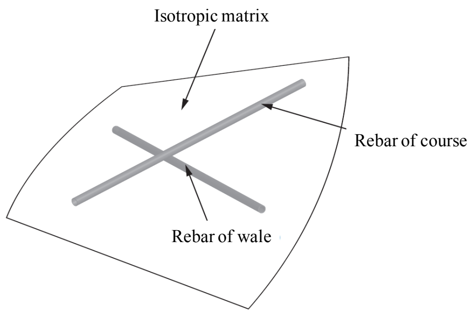

Figure 3. Schematic diagram of a shell with rebar.

2.2 Formulation of anisotropic hyperelastic material model

Although the rebar layer model is easy to assemble, it is not suitable for more accurate fabric modeling of the interaction between the wale and course. Taking this interactive effect into account, an anisotropic hyperelastic material model (Tanaka et al. 2010) is proposed in this section. The strain energy function applied to this material model is formulated so that the polyconvexity condition is satisfied as per suggestions by Schroder (2005) and Itskov (2006). For a boundary value problem, the strain energy functions W are required to satisfy the four conditions below so that robust and physically meaningful analysis can be performed.

1. Continuity condition
2. Energy- and stress-free natural state condition
3. Polyconvexity condition
4. Growth condition

Condition 1 indicates that at least the C2-continuity of the strain energy function should be held in order to compute the stress and tangent stiffness. Condition 2 refers to the necessity of an energy- and stress-free state in the reference configuration for a finite elasticity boundary value problem. Condition 3 is defined so that if there exists a convex function W with respect to the deformation gradient tensor $\mathbf{F}$, cofactor of $\mathbf{F}$ (denoted as cof $\mathbf{F}$), and Jacobian J = det $\mathbf{F}$, the strain energy function can be regarded as being polyconvex. Condition 4 refers to the coercivity. The polyconvexity with its continuity and coercivity is sufficient to ensure the existence of the global minimizer of the total elastic energy.

Considering these conditions, the strain energy function W of the anisotropic hyperelastic models can be given in terms of the right Cauchy-Green deformation tensor $\mathbf{C} = \mathbf{F}^T\mathbf{F}$ and a new tensor $\mathbf{M}_i$ with the form:

$$W = W(\mathbf{C}, \mathbf{M}_i) \tag{5}$$

$\mathbf{M}_i$ is the so-called structural tensors denoted as

$$\mathbf{M}_i = \mathbf{n}_i \otimes \mathbf{n}_i \tag{6}$$

$\mathbf{n}_i$ is the unit base vector in the principal material directions, as indicated by the 2-D example in Figure 4 and $\otimes$ represents the tensor product. Now, i represents the index of the fiber or the principal material direction, and the summation convention is not employed in this equation.

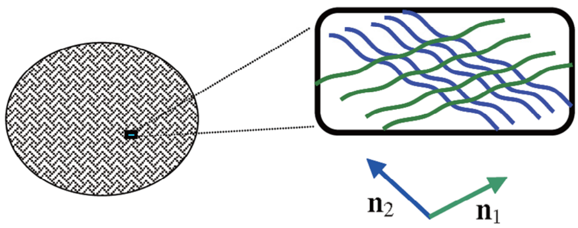

Figure 4. Structural tensor $\mathbf{M}_i$.

In this study, the following polyconvex strain energy function W for orthotropic incompressible hyperelastic materials, developed by Itskov (2006), is utilized for modeling of cloth behavior.

$$W = \frac{1}{4}\sum_{r}^{N}\mu_r\left[\frac{1}{\alpha_r}(\tilde{J}_r^{\alpha_r} - 1) + \frac{1}{\beta_r}(\tilde{K}_r^{\beta_r} - 1)\right] \tag{7}$$

where N(positive integer), $\mu_r > 0$, $\alpha_r \geq 1$, and $\beta_r \geq 1$ are material constants, and $\tilde{J}_r$ and $\tilde{K}_r$ are generalized pseudo invariants defined as follows:

$$\tilde{J}_r \equiv \mathrm{tr}(\mathbf{C}\tilde{\mathbf{M}}_r), \quad \tilde{K}_r \equiv \mathrm{tr}(\mathrm{cof}(\mathbf{C})\tilde{\mathbf{M}}_r) \tag{8}$$

$0 \leq w_i^{(r)} \leq 1$

where $\tilde{\mathbf{M}}_r$ is the generalized structural tensor given by

$$\tilde{\mathbf{M}}_r \equiv w_1^{(r)}\mathbf{M}_1 + w_2^{(r)}\mathbf{M}_2 + w_3^{(r)}\mathbf{M}_3 \tag{9}$$

$w_r^{(r)}$ represents the weight factors of the principal material directions and $w_r^{(r)}$ determines the effect of the interaction between fibers. The weight factors $w_r^{(r)}$ take values between 0 and 1, as given in Equation (10), and the higher the value of $w_r^{(r)}$, the stronger is the effect of the fiber of direction i on the others. This feature enables to obtain the expression of directional anisotropy. Note that when all $w_r^{(r)}$ take values equal to 1/3, the material behaves isotropically.

$$0 \leq w_i^{(r)} \leq 1 \tag{10}$$

The strain energy function satisfies the four prerequisite conditions mentioned in the previous section so no additional restrictions should be imposed on the associated material coefficients. These coefficients can be evaluated on the basis of experimental data. The material model of Equation (7) is implemented in Abaqus/Standard by using the UMAT user-defined material subroutine. Components of the Cauchy stress and the tangent stiffness matrix, called the “material Jacobian” in Abaqus/Standard, are required to return to the main program.

Although the present material model is formulated with the total Lagrangian description associated with the second Piola-Kirchhoff stress, the stress can be transformed into the Cauchy stress. To specify the material Jacobian correctly, the component values have to be chosen and computed depending on the type of finite element and objective stress rate being used. Abaqus/Standard uses the Green-Naghdi rate of Kirchhoff stress and rate-of-deformation tensor for structural elements such as shells, membranes, beams, and trusses. Therefore, the tangent modulus related to the Green-Naghdi rate of the Kirchhoff stress tensor and rate-of-deformation tensor have to be given. To implement the derived material model in the shell elements, the additional plane stress condition and appropriate thickness update should be accounted. In this study, an incompressible deformation is assumed to simplify the calculation of the thickness change. The initial thickness is 1 mm.

3. Parameter identification of material models and pantyhose analysis

In this section, the material parameters for the rebar layer model and the anisotropic hyperelastic model are numerically identified. To identify the material parameters, three uniaxial tensile tests in three directions: wale, course, and bias at an angle of 45 are performed, as shown in Figure 5. To fit the stress-strain relationships with the experimental data in all three directions, the material constants are determined using genetic algorithm (GA). Figure 6 shows the results from the tensile tests made for the cloth material that exhibits highly anisotropic behavior typically used for the products like pantyhose and tights. The material constants identified for the rebar layer model and the anisotropic hyperelastic model are shown in Table 1 and Table 2 respectively.

Figure 6 shows the analytical results using these material constants. The tensile stresses in the wale and the course directions could be successfully simulated by the analysis with either of the material models (Figure 6(a) and (b)). On the other hand, the stretching along the bias shows a remarkable interaction between the wale and the course (Figure 6(c)). The deformed shape looks very distorted and higher stress is induced in the high-strain regions. As the anisotropic hyperelastic model contains the material parameters that allow this interactive behavior, the increase in the stress can be correctly represented by this model. The rebar layer model is not capable of representing the increase in the stress because this model does not take such interaction into account. The tensile test specimen is clamped at both ends and necking deformation due to elongation is produced in the mid-portion of the test specimen. This necking reflects the interaction between the wale and the course, and therefore the analysis with the anisotropic hyperelastic model may give a better approximation.

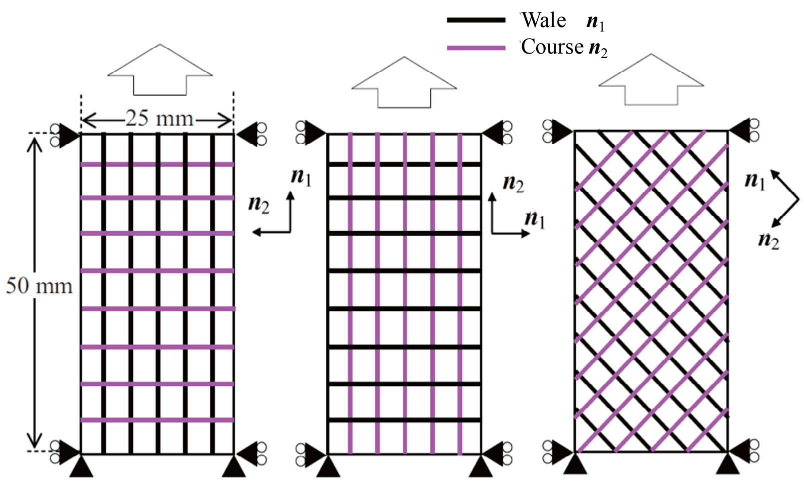

Figure 5. Simple tensile tests of knitted strips.

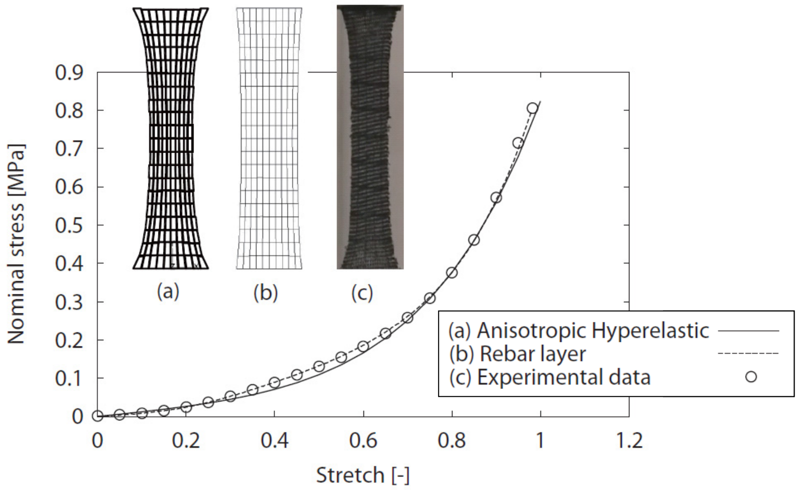

(a) Wale direction

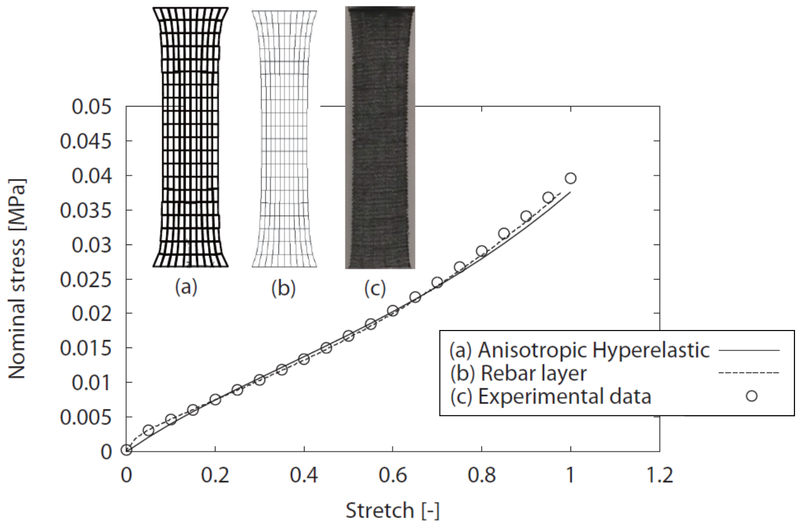

(b) Course direction

Figure 6. Stress-strain curves of pantyhose fabric test specimen.

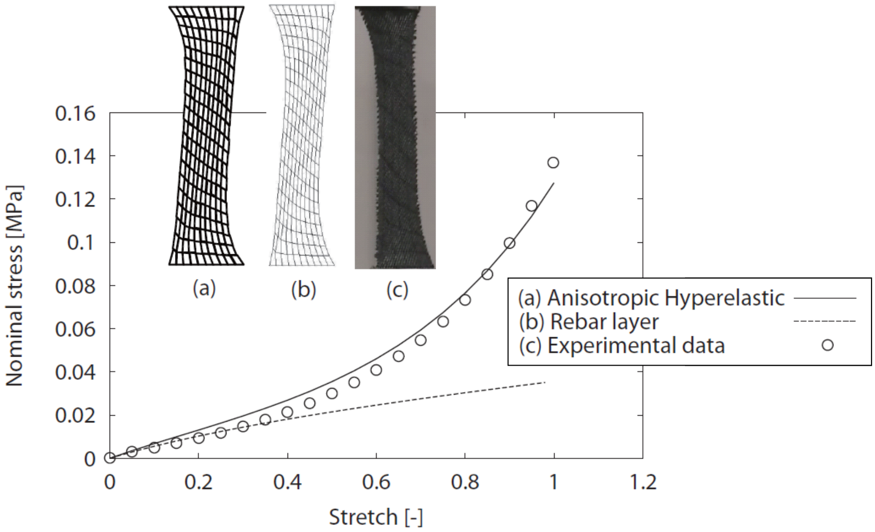

(c) Bias direction

Figure 6 (cont.). Stress-strain curves of pantyhose fabric test specimen.

Table 1. Material parameters of pantyhose fabric for rebar layer model.

C_{10}
8.4667×10^{-3} MPa

c_0	c_1	c_2	c_3	c_4	c_5
0.0001 MPa	0.1672 MPa	−2.225 MPa	21.199 MPa	−62.05 MPa	61.746 MPa
d_0	d_1	d_2	d_3	d_4	d_5
0.0032 MPa	−0.075 MPa	0.4653 MPa	−1.340 MPa	1.9400 MPa	−0.986 MPa

Table 2. Material parameters of pantyhose fabric for anisotropic hyperelastic model.

μ_1	μ_2	μ_3
1.2755×10^{-2} MPa	2.0569×10^{-3} MPa	4.5867×10^{-2} MPa

α_1	α_2	α_3	β_1	β_2	β_3
4.727	1.475	1.736	1.003	16.16	1.063
$w_1^{(1)}$	$w_2^{(1)}$	$w_1^{(2)}$	$w_2^{(2)}$	$w_1^{(3)}$	$w_2^{(3)}$
0.771	0.229	0.585	0.415	0.652	0.348

Figures 7 and 8 illustrate the analytical results for the clothing pressure in the case of putting on pantyhose. The pantyhose fabric exhibits remarkable anisotropic behavior (Figure 6). The anisotropic hyperelastic model is still only applicable to the level of tensile test specimen, and any successful application of this type of model to real pantyhose has not been reported as of the date of this study. The results in Figures 7 and 8 are derived from the analysis of the rebar layer model. The human leg has a relatively simple geometric shape when standing upright and pressure generated on pantyhose is governed by the curvature circumferentially around the leg. Therefore, the rebar layer model has sufficient accuracy that meets practical purposes. Actually, as shown in Figure 8, the matching of the analytical results with the experimental results appears to be good.

For reference, the appended graph in gray shows the results from another analysis in which the material property of the cloth was changed from the original anisotropic property to the hypothetical isotropic behavior. These results differ significantly. The method developed in this study is utilized as a tool with enough practicability for the design of pantyhose. The analysis technique of the clothing process will be described in the following section.

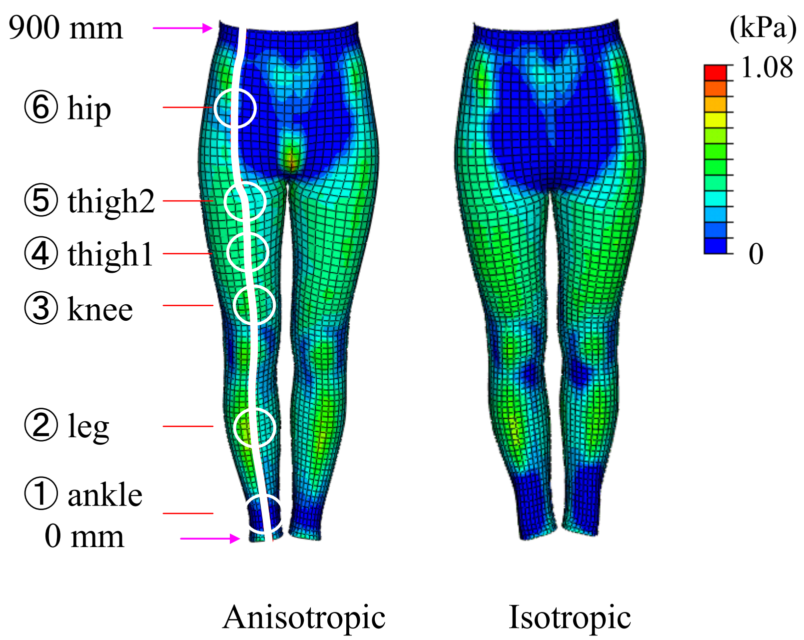

Figure 7. Pantyhose pressure distribution analysis (Comparison between anisotropic and isotropic material models).

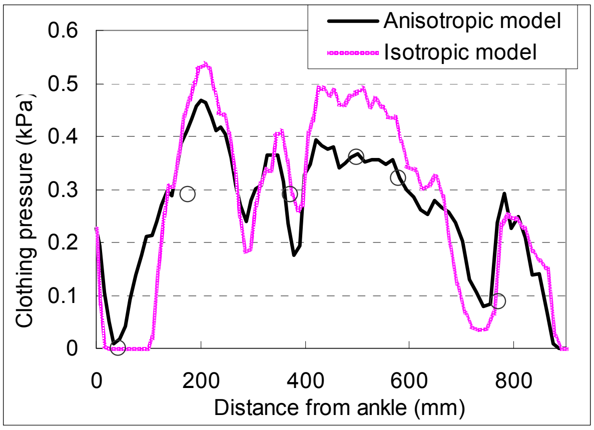

Figure 8. Pantyhose pressure distribution from ankle to waist.

4. Prediction of clothing pressure for T-shirt

A three-dimensional finite element analysis was carried out using Abaqus/Standard to obtain the distribution of clothing pressure acting on a human body. The analyzed cloth is meshed with the four-node shell elements (S4R in Abaqus/Standard) and the objects chosen in this simulation were T-shirt fabrics. The material parameters of the T-shirts were determined by the numerical identification in Table 3 for the rebar layer model and the anisotropic hyperelastic model in Table 4. Figure 6 shows the stress-strain curves derived from the analysis using the material parameters listed in Tables 3 and 4. The degree of the anisotropic property of the T-shirt fabrics was not as remarkable as the cloth of the pantyhose.

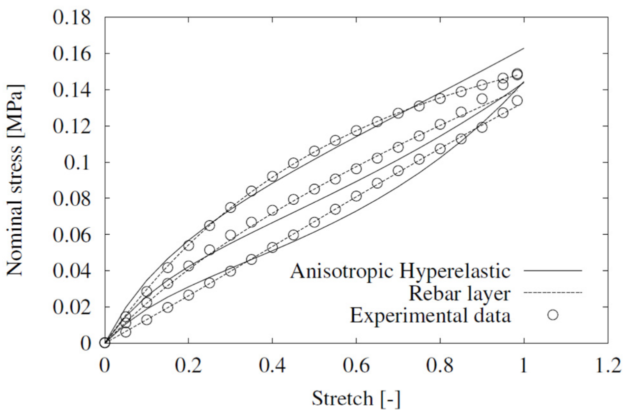

Figure 9. Load-displacement curves of T-shirts fabric test specimen.

Table 3. Material parameters of T-shirts for rebar layer model.

C_{10}	c_0	c_1	c_2	c_3
3.82×10^{-2}MPa	0.0064 MPa	0.0786 MPa	−0.287 MPa	0.2156 MPa

d_0	d_1	d_2	d_3
−0.010 MPa	0.0206 MPa	0.0291 MPa	−0.013 MPa

Table 4. Material parameters of T-shirts for anisotropic hyperelastic model.

μ_1	μ_2	μ_3
6.8837×10^{-3} MPa	8.6240×10^{-2} MPa	1.2354×10^{-1} MPa

α_2	α_3	α_3	β_1	β_2	β_3
3.52	1.28	1.00	1.004	13.49	1.002

$w_1^{(1)}$	$w_2^{(1)}$	$w_1^{(2)}$	$w_2^{(2)}$	$w_1^{(3)}$	$w_2^{(3)}$
0.321	0.565	0.585	0.435	0.781	0.219

The mannequin used in this simulation corresponded to the average body of a 20-year-old Japanese woman (Figure 10). Pressure sensors were used to measure contact pressure between the cloth and the mannequin's surface. This experimental system served to obtain point-to-point measurement data and such observations can hardly predict the overall distribution of contact pressure on a human body. To overcome this problem, a numerical simulation using a nonlinear FEM was conducted. In this study, the human body was modeled using rigid elements. Because the surface of the mannequin was sufficiently smooth to avoid the occurrence of any excessive tensions or wrinkles on the clothing during the experiment, the friction between the cloth and the human body was not considered in the simulation.

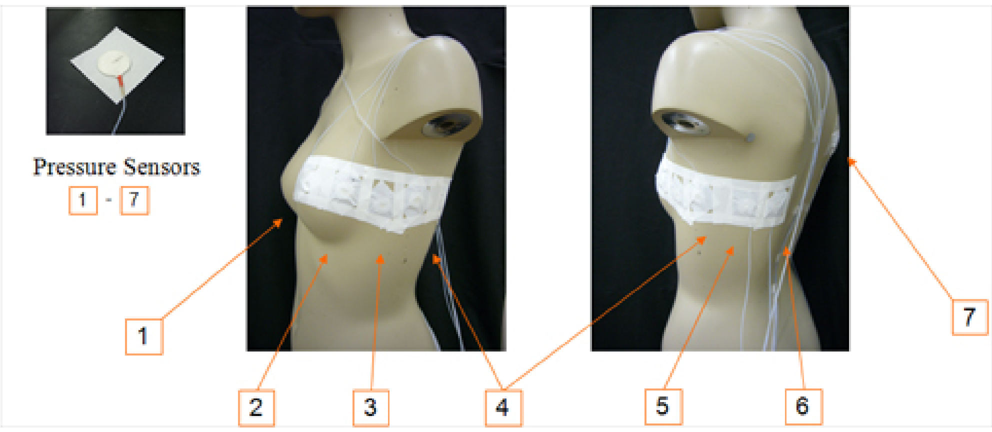

Figure 10. Measurement of clothing pressure on mannequin.

Figure 11 shows the clothing process of the simulation (INSIGHTS, 2009). Prior to sewing, the T-shirt was segmented into four parts: front bodice, back bodice, left sleeve, and right sleeve. Each of these parts was modeled based on geometry in accordance with the dimensions given by the respective dress pattern and located at the specified position around the mannequin. The clothing process progressed in such a way that the cloth parts were stretched by imposing the enforced displacement on the nodes that composed the stitch line, and each part was gently gathered to cover the surface of the mannequin. The nodes to be stitched were guided to the same position by enforced displacement so that these nodes were tied to each other. After sewing was completed, the enforced displacement imposed on each node was released, so that the T-shirt began to deform to fit the surface of the mannequin and rest at a stable equilibrium state. The CPU time was around two hours on an average PC.

Figure 11 (right) shows the shape obtained at the stable state. While an enforced displacement was imposed on each part, the cloth was mostly subjected to tensile stresses, but wrinkles occurred in some parts during the fitting phase Figure 11 shows that the cloth around the waist of the mannequin was actually wrinkled. From the viewpoint of structural analysis, such deformation can be regarded as local buckling. The material model employed in this study was formulated with the constitutive law in the behavior under tension, but the stiffness against compression was set to zero. Accordingly, along with the occurrence of the local buckling, this was likely to lead to a numerical instability state. In Abaqus/Standard, the special feature for stabilizing the analysis steps introduced the artificial damping effect. In this study, this capability was applied to the clothing process so that a fully automated analysis could be performed.

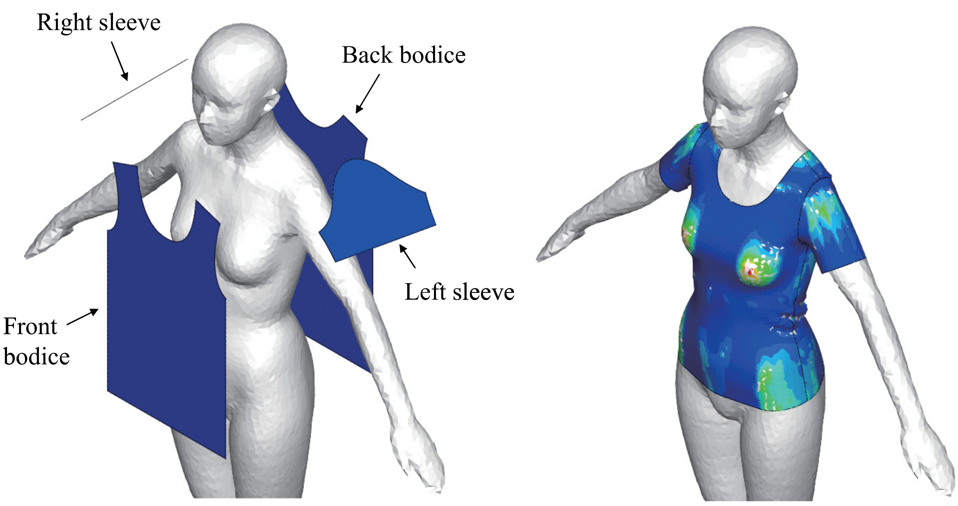

Figure 11. Clothing process simulation.

Figure 12 shows the contour plot of the contact pressure distributed over the mannequin's surface. As the curvature along the back of the human body is small, the intensity of the clothing pressure is likely to be reduced and the pressure tends to concentrate onto the protuberance of shoulder blade. In the case of the shirts specifically designed for athletes, optimizing the pressure distribution was contrived by changing the cloth material from part to part. Figure 13 shows the clothing pressure distributed along the bust line. The match between the analytical results and the experimental measurements was good.

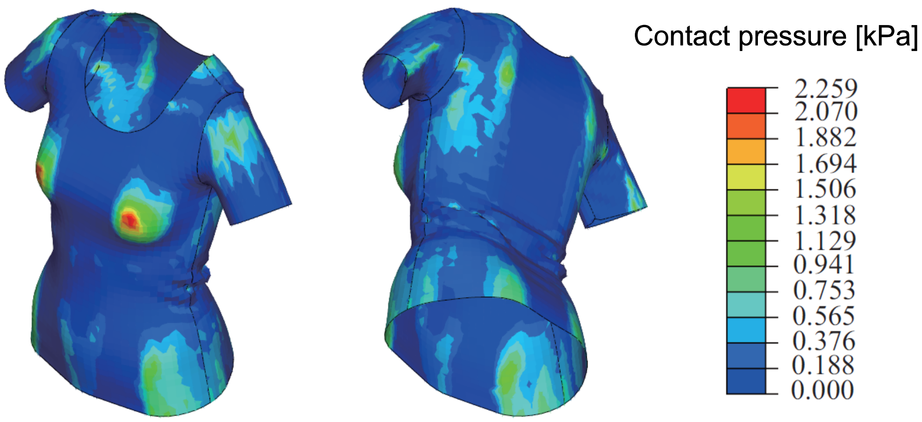

Figure 12. Clothing pressure distribution.

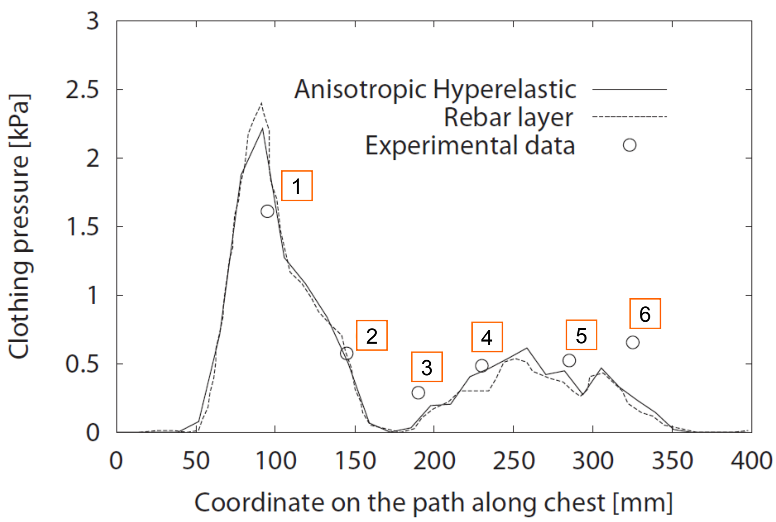

Figure 13. Clothing pressure distribution along the bust line.

Compared with the analysis for the pantyhose, the T-shirt clothing process is more complicated, but the anisotropic property of the cloth material is not dominant, so the analysis could be carried out using either the rebar layer model or the anisotropic hyperelastic model. In contrast to the results obtained with the rebar layer model, those obtained with the anisotropic hyperelastic model were in good agreement with the measurements, especially under the armpits (at observation points 4 and 5). Such a difference was generated due to the human body around this region forming a three dimensionally complex shape.

5. Conclusion

This study presents the implementation of two material models to predict the mechanical behavior of cloth. One was the rebar layer model that consisted of the isotropic hyperelastic matrix part and the reinforcing rebar layer part. The other was the polyconvex anisotropic hyperelastic model. The effect of the interaction between the fibers in the wale and course orientations was considered as weighted factors. The simulation successfully computed the pressure exerted by clothing on a mannequin, and good agreement with the experimental data was realized. In the future, we intend to incorporate the biaxial tension test for knitted fabric and the material model in our study.

Acknowledgements

This research was strongly supported by the Technology Development Foundation for Rational Use of Energy (Next Generation Technology Development for Rational Use of Energy concerning Fabrics or Development of Fiber Products that induce Physical and Mental Comfort), in METI, Japan. The authors wish to express their thanks to all the contributors. The late Professor Hirohisa Noguchi of Keio University greatly contributed with his suggestions and guidance to this study until immediately before he passed away on August 22, 2008.

6. References

1. Ishimaru,S., Isogai,Y., Matsui,M., Furuichi,K., Nonomura,C.and Yokoyama,A, “Method for Clothing Pressure Distribution by Numerical Approach”, Textile Research Journal (submitted for publication).
2. Itskov, M., Ehret, A. E., and Mavrilas, D., “A polyconvex anisotropic strain energy function for soft collagenous tissues”, Biomech Model Mechanbiol, vol. 5, pp. 17–26, 2006.
3. Schröder, J., Neff, P., and Balzani, D., “A variational approach for materially stable anisotropic hyperelasticity”, International Journal of Solids and Structures, vol. 42, pp. 4352–4371, 2005.
4. Tanaka, M., Noguchi, H., Fujikawa, M., Sato, M., Oi, S., Kobayashi, T., Furuichi, K., Ishimaru, S., and Nonomura, C., “Development of Large Strain Shell Elements for Woven Fabrics with Application to Clothing Pressure Distribution Problem”, CMES, vol.62, no.3, pp.265-290, 2010.
5. Yeung, K.W., Li, Y., Zhang, X., J.Text.Inst., 95, 59-79, 2004.
6. Dassault Systems Simulia Corp., “Designing COMFORT into clothing”, INSIGHTS, May/June, pp.16-18, 2009.